Contents lists available at ScienceDirect

Materials Letters

The effect of P on the glass forming ability and soft magnetic properties of Co–Fe–P–Si–B–C–Mo bulk glassy alloys

Huaijun Sun [a,*], Li Li [a], Yunzhang Fang [a], Linlin Wang [b], Xindu Fan [c], Baolong Shen [c]

[a] College of Physics, Mathematics and Information Engineering, Zhejiang Normal University, Jinhua 321004, China
[b] College of Engineering, Zhejiang Normal University, Jinhua 321004, China
[c] School of Materials Science and Engineering, Southeast University, Nanjing 210018, China

ARTICLE INFO

ABSTRACT

Co-based bulk ferromagnetic glassy alloys with diameters up to 5 mm were formed in $Co_{45.6}Fe_{30.4}P_x$-$Si_{11.4-x}B_{6.6}C_4Mo_2$ system by the copper mold casting method. The effect of P addition on the glass-forming ability (GFA) and soft magnetic properties in the alloys system was investigated. In addition to the increase of glass-forming ability, increasing P content was found to be effective for the improvement of soft-magnetic properties. The bulk glassy alloys exhibit excellent soft-magnetic properties, i.e., high saturation magnetization of 1.08 T, low coercive force within 2.0–3.4 A/m, high permeability of 15795 at 1 KHz, and Curie temperature of 665–694 K. The successful synthesis of the $Co_{45.6}Fe_{30.4}P_x$-$Si_{11.4-x}B_{6.6}C_4Mo_2$ bulk glassy alloys system exhibiting high GFA and good soft-magnetic properties is encouraging for the future applications of structural and functional materials.

1. Introduction

The developments of Fe- and Co-based bulk glassy alloys (BGAs), especially for Fe-based BGAs, have been drawing increasing attention due to their good soft-magnetic properties and superhigh fracture strength in this one decade, which are potential for using as functional and structural materials [1–14]. Among them, although the Co-based BGAs exhibit excellent soft-magnetic properties and high fracture strength (σ_f), they have not been noticed so widely as compared with the Fe-based BGAs because of their low glass-forming ability (GFA) and low saturation magnetization (I_s). Recently, Fe–(P, C)-based BGAs with a small amount of metalloid have been developed by varying the composition [15–20]. These alloys have attracted specific attention due to not only their unique combination of excellent GFA, high I_s, high fracture and good corrosion resistance, but also the low cost resulting from plentiful natural resources of Fe element on the earth. Meanwhile, Minor alloying effects of Nb and Mo on the thermal stability and magnetic properties of these alloys have been investigated extensively [19–23], while there are few reports about the effects of P addition on glassy alloys up to now.

In recent years, with the aim of synthesizing CoFeBSi glassy alloys with high GFA and excellent soft-magnetic properties, we modified the B, Si and Nb contents, synthesized $(Co_{0.89}Fe_{0.057}Nb_{0.053})_{72}$ $(B_{0.8}Si_{0.2})_{28}$ and $(Co_{0.942}Fe_{0.058})_{67}Nb_5B_{22.4}Si_{5.6}$ BGAs. They exhibit low H_c of 0.4 and 0.2 A/m, respectively, and higher GFA, but remained an unresolved problem of low I_s of 0.51 and 0.43 T, respectively [13,14]. Therefore, just modifying the contents of the B, Si and Nb additions cannot meet the needs to simultaneously increase the GFA and soft-magnetic properties. In this study, Co-based BGAs $Co_{45.6}Fe_{30.4}P_x$-$Si_{11.4-x}B_{6.6}C_4Mo_2$ with diameters in the range up to 5 mm were synthesized. This glassy alloy system exhibited high saturation magnetization (I_s) of 1.08 T, low coercive force (H_c) of 2.0–3.4 A/m, high effective permeability (μ_e) of 15,795 at 1 kHz under a field of 1 A/m and Curie temperature of 665–694 K.

2. Experiment

Alloy ingots with nominal compositions of $Co_{45.6}Fe_{30.4}P_x$-$Si_{11.4-x}B_{6.6}C_4Mo_2$ ($x = 5$, 5.5, 6, 6.5, 7 and 7.5) (at%) were made by alloying pure Co (99.9 mass%), Fe (99.9 mass%), Mo (99.9 mass%), C (99.9 mass%), B (99.9 mass%) and Si (99.9 mass%), and pre-alloyed Fe–P ingots under a high-purity argon atmosphere. Ribbons with thickness of 20 μm and width of 1.2 mm were prepared by the single copper roller melt-spinning method. Cylindrical alloy rods with diameters of 1–6 mm were produced by copper mold casting.

* Corresponding author. Tel.: +86 579 82298852.
E-mail address: shj@zjnu.cn (H. Sun).

Those alloy rods were sectioned by a fine cutter, and the transverse cross sections were examined by X-ray diffraction (XRD) with Cu $K\alpha$ radiation. Thermal stability associated with glass transition temperature (T_g), crystallization temperature (T_x), and supercooled liquid region ($\Delta T_x = T_x - T_g$) was examined by differential scanning calorimetry (DSC) at a heating rate of 0.67 K/s. The liquidus temperature (T_l) was measured by cooling the molten alloy samples with a DSC at a cooling rate of 0.067 K/s. I_s was measured with a vibrating sample magnetometer (VSM) under an applied field of 800 kA/m. H_c was measured with a B–H loop tracer under a field of 800 A/m. μ_e from 1 to 100 kHz was measured with an impedance analyzer under a field of 1 A/m. As the magnetic properties are affected with the sample sizes, so that to clarify the intrinsic soft-magnetic properties of this Co-based glassy alloy system, ribbon samples with the same size as mentioned above were used for measurement. All of the samples for magnetic property measurements were annealed for 300 s at the temperature of $T_g - 50$ K for improving soft-magnetic properties through structural relaxation.

3. Results and discussion

Fig. 1 (a) shows DSC curves of the melt-spun $Co_{45.6}Fe_{30.4}P_x$-$Si_{11.4-x}B_{6.6}C_4Mo_2$ glassy alloy ribbons. It is seen that all of the alloys exhibit distinct glass transition, followed by a supercooled liquid region, and then crystallization. It is also seen that these glassy alloys have a ferromagnetic state and the transition from ferromagnetic to paramagnetic states occurs at 665–694 K, as marked with T_c. With the P content increase gradually from 5 to 7.5 at%, ΔT_x increase from 35 to 50 K. The onset and end

temperatures of glass transition are marked as T_g^{onset} and T_g^{end}, respectively. For these glassy alloys, it is clearly seen that the difference of specific heat (ΔC_p) between the onset and end of glass transition increases with increasing the P content. The value of ΔC_p at the glass transition region (i.e., between temperature range of T_g^{onset} and T_g^{end}) indicates how much different the structure changes are at the glass transition. Indeed, the glass transition becomes more distinguished with increasing the P content as shown in the DSC curves. Thus, it is considered that the thermal stability of the supercooled liquid increases with increasing the P content.

We have also examined the composition dependence of the reduced glass transition temperature (T_g/T_l). As shown in Fig. 1(b),
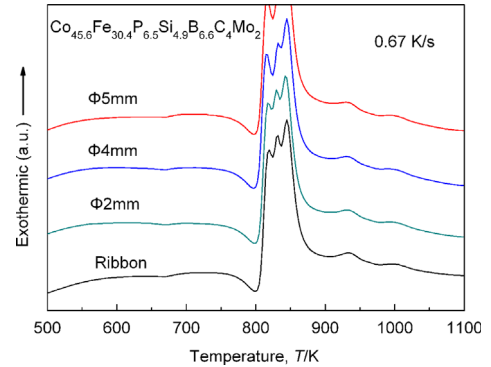
Fig. 3. DSC curves of the $Co_{45.6}Fe_{30.4}P_{6.5}Si_{4.9}B_{6.6}C_4Mo_2$ glassy alloy rods with diameters of 2, 4 and 5 mm, together with the data for the melt-spun glassy alloy ribbon for comparison.
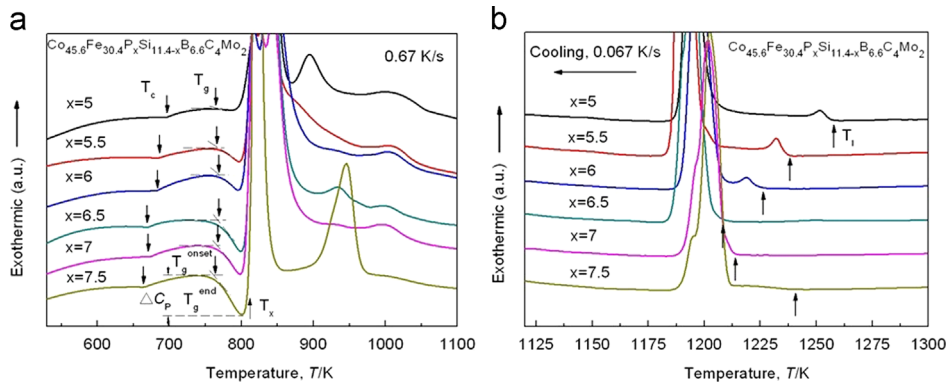
Fig. 1. (a) DSC curves of melt-spun $Co_{45.6}Fe_{30.4}P_xSi_{11.4-x}B_{6.6}C_4Mo_2$ (x=5, 5.5, 6, 6.5, 7 and 7.5) glassy alloy ribbons. (b) DSC curves of $Co_{45.6}Fe_{30.4}P_xSi_{11.4-x}B_{6.6}C_4Mo_2$ (x=5, 5.5, 6, 6.5, 7 and 7.5) alloys.
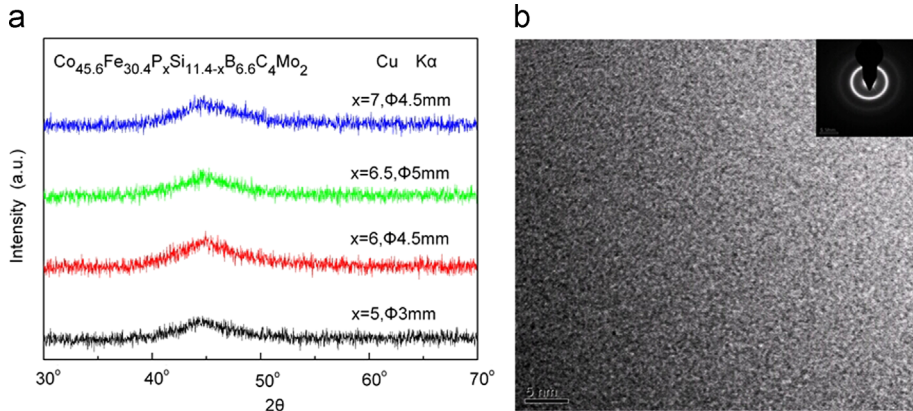
Fig. 2. (a) XRD patterns of the cast $Co_{45.6}Fe_{30.4}P_xSi_{11.4-x}B_{6.6}C_4Mo_2$ (x=5, 6, 6.5 and 7) alloy rods with diameters of 3, 4.5, 5, and 4.5 mm. (b) HRTEM image of the as-cast $Co_{45.6}Fe_{30.4}P_{6.5}Si_{4.9}B_{6.6}C_4Mo_2$ glassy alloy. The inset displays the corresponding selected area electron diffraction (SAED) pattern.

Table 1

Maximum diameter, thermal stability, and magnetic properties of cast $Co_{45.6}Fe_{30.4}P_xSi_{11.4-x}B_{6.6}C_4Mo_2$ ($x=5$, 5.5, 6, 6.5, 7, 7.5) glassy alloy rods.

Alloy	D_{max} (mm)	Thermal stability							Magnetic properties		
		T_g (K)	T_x (K)	ΔT_x (K)	T_c (K)	T_l (K)	T_g/T_l	ΔC_P (J/(g K))	I_s (T)	H_c (A m^{-1})	μ_e (1 KHz)
$Co_{45.6}Fe_{30.4}P_5Si_{6.4}B_{6.6}C_4Mo_2$	3	763	798	35	694	1256	0.607	0.015	1.08	3.4	9018
$Co_{45.6}Fe_{30.4}P_{5.5}Si_{5.9}B_{6.6}C_4Mo_2$	3.5	764	801	37	684	1237	0.618	0.075	1.07	3.1	10,849
$Co_{45.6}Fe_{30.4}P_6Si_{5.4}B_{6.6}C_4Mo_2$	4.5	765	803	38	684	1224	0.625	0.167	1.04	2.9	10,906
$Co_{45.6}Fe_{30.4}P_{6.5}Si_{4.9}B_{6.6}C_4Mo_2$	5	766	805	39	671	1202	0.637	0.376	1.07	2.0	15,795
$Co_{45.6}Fe_{30.4}P_7Si_{4.4}B_{6.6}C_4Mo_2$	4.5	765	805	40	674	1209	0.632	0.396	1.07	2.5	14,485
$Co_{45.6}Fe_{30.4}P_{7.5}Si_{3.9}B_{6.6}C_4Mo_2$	4.5	764	814	50	665	1243	0.611	0.421	1.04	2.8	11,872

the T_l decreases from 1256 to 1202 K with an increase of P content from 5% to 6.5%, resulting in the increase of T_g/T_l from 0.607 to 0.637. This result indicates that higher glass-forming ability may be obtained by increasing P content. However, when P contents increase to 7.5%, as can be seen in Fig. 1(b), the T_l increases to 1243, and the T_g/T_l decreases to 0.611 accordingly, glass-forming ability also begins to decrease with it.

Based on the results obtained from DSC measurements, it is considered that this Co-based glassy alloy system may exhibit high GFA. Then, we tried to form cylindrical glassy rods with different diameters up to 6 mm. The glassy alloy rods were produced at all alloy compositions in this system. The critical diameter for the formation of a glassy single phase was 3 mm at $x=5$, 3.5 mm at $x=5.5$, 4.5 mm at $x=6$, 5 mm at $x=6.5$, 4.5 mm at $x=7$, and 4.5 mm at $x=7.5$. Fig. 2(a) shows XRD patterns of those cast alloy rods. Only broad peaks without a crystalline peak can be seen for all of these bulk samples, indicating the formation of a glassy phase in the diameter range up to 5 mm. Tranmission electron microscopy (TEM) images and the corresponding selected-area electron diffraction patterns confirm the amorphous character of the as-cast alloy (Fig. 2(b)). The DSC examination results also denote the formation of a glassy phase. As one of the DSC examination results, Fig. 3 shows DSC curves of the $Co_{45.6}Fe_{30.4}P_{6.5}Si_{4.9}B_{6.6}C_4Mo_2$ glassy alloy rods with diameters of 2, 4, and 5 mm, respectively, together with the data for the melt-spun glassy alloy ribbon. It is seen that the bulk alloys exhibit a distinct glass transition at 766 K, followed by a supercooled liquid region of 42 K. No appreciable difference in T_g, T_x, ΔT_x, or crystallization process was observed between the melt-spun ribbon and rod samples. The XRD and DSC measurement results indicate clearly the formation of the Co-based glassy alloy rods with diameters in the range up to 5 mm.

Table 1 summarizes the maximum diameter, thermal stability, and magnetic properties of the $Co_{45.6}Fe_{30.4}P_xSi_{11.4-x}B_{6.6}C_4Mo_2$ ($x=5$, 5.5, 6, 6.5, 7 and 7.5) (at%) glassy alloys. In addition to high GFA, this BGA system also exhibits good soft-magnetic properties, i.e., high saturation magnetization of 1.08 T, low coercive force within 2.0–3.4 A/m, high permeability of 15,795 at 1 KHz, and Curie temperature of 665–694 K.

As described above, the network-like structure of the $Co_{45.6}Fe_{30.4}P_xSi_{11.4-x}B_{6.6}C_4Mo_2$ glassy alloy becomes strong with increases of the P content. As a result, the thermal stability of the supercooled liquid against crystallization increased, as can be confirmed from the increases of ΔC_p and T_g as shown in Fig. 1(a). In this study, the atomic radii of Co, Fe, Mo, B, P and Si are 0.125, 0.124, 0.136, 0.09, 0.109 and 0.117 nm, respectively [24]. It has been pointed out that the large (L) and small (S) atoms may form a strong L–S percolating network or reinforced 'backbone' in the amorphous structure [25]. Therefore, it is considered that the bonding nature of the network-like structure increases with alternative Si with P, resulting in enhancing the stability of the undercooled liquid, which further suppresses crystallization. On the other hand, the enthalpy of mixing is −31 kJ/mol for the P–Fe pair, −27 kJ/mol for the P–Co pair, −45 kJ/mol for the P–Mo pair, −18 kJ/mol for the Si–Fe pair,

−21 kJ/mol for the Si–Co pair, −18 kJ/mol for the Si–Mo pair [26]. It can be seen that there are larger mixing enthalpies with negative values in the atomic pairs between P and Co, Fe and Mo, respectively, and the mixing enthalpy with negative values of the P–Mo atomic pair is as large as 45 kJ/mol. Lastly, the appropriate increase of the P content effectively causes the approaching of alloy composition to the eutectic point as shown in Fig.1(b). However, when the P content was more than 6.5 at%, the composition will deviate from the eutectic point again, and the T_g/T_l will decrease with it, accordingly, the GFA will also begin to decrease. The origin of the high μ_e can be attributed to the low number density of the domain-wall pinning sites [27], resulting from the high degree of amorphicity and structural homogeneity proceeding from the high GFA [28]. Consequently, the increase of the thermal stability of the supercooled liquid and the approaching phenomenon to a eutectic point by adjusting the P content lead to the high GFA and excellent soft-magnetic properties.

4. Conclusions

In conclusion, a BGA system $Co_{45.6}Fe_{30.4}P_xSi_{11.4-x}B_{6.6}C_4Mo_2$ with high GFA, high saturation magnetization and good soft-magnetic properties was synthesized. This Co-based ferromagnetic glassy alloy system is promising for the future applications as functional materials.

References

[1] Inoue A, Shen BL. Mater Trans 2002;43:766.
[2] Ponnambalam V, Poon SJ, Tayloy R, Petculescu G. Appl Phys Lett 2003;83:1131.
[3] Inoue A, Shen BL, Koshiba H, Kato H, Yavari AR. Nat Mater 2003;2:661.
[4] Ponnambalam V, Poon SJ, Shiflet GJ. J Mater Res 2004;19:1320.
[5] Lu ZP, Liu CT, Thompson JR, Porter WD. Phys Rev Lett 2004;92:245503.
[6] Wang WH, Pan MX, Zhao DQ, Bai HY. J Phys Condens Matter 2004;16:3719.
[7] Shen BL, Inoue A, Chang CT. Appl Phys Lett 2004;85:4911.
[8] Chang CT, Kubota T, Makino A, Inoue A. J Alloys Compd 2009;473:368.
[9] Chang CT, Shen BL, Inoue A. Appl Phys Lett 2006;88:011901.
[10] Kim DH, Park JM, Kim DH, Kim WT. J Mater Res 2007;22:471.
[11] Yao JH, Wang JQ, Li Y. Appl Phys Lett 2008;92:251906.
[12] Bitoh T, Shibata D. J Appl Phys 2009;105:07A312.
[13] Sun HJ, Man QK, Dong YQ, Shen BL, Inoue A. J Alloys Compd 2010;504S:31.
[14] Sun HJ, Man QK, Dong YQ, Shen BL, Inoue A. J Appl Phys 2010;107:09A319.
[15] Liu FJ, Pang SJ, Li R, Zhang T. J Alloys Compd 2009;483:613.
[16] Liu FJ, Yang QW, Pang SJ, Zhang T. J Non-Cryst Solids 2009;355:1444.
[17] Zhang W, Fang CF, Li YH,. Scripta Mater. 2013;69(1):77.
[18] Wang JF, Li R, Hua NB, Huang L, Zhang T. Scripta Mater. 2011;65:536.
[19] Li X, Qin CL, Kato H, Makino A, Inoue A. J Alloys Compd 2011;509:7688.

[20] Yang XH, Ma XH, Li Q, Guo SF. J Alloys Compd 2013;554:446.
[21] Guo SF, Shen Y. Trans Nonferr Metals Soc China 2011;21:2433.
[22] Li HX, Kim KB, Yi S. Scripta Mater. 2007;56:1035.
[23] Jung HY, Yi S. Intermetallics 2010;18:1936.
[24] Metals Databook. Maruzen, Tokyo: The Japan Institute of Metals; 2004. p. 8.

[25] Poon SJ, Shiflet GJ, Guo FQ, Ponnambalam V. J Non-Cryst Solids 2003;317:1.
[26] De Boer FR. Cohesion in metals. Amsterdam: North-Holland; 1989; 217.
[27] Bitoh T, Makino A, Inoue A. J Appl Phys 2006;99:08F102.
[28] Inoue A. Mater Sci Eng A 2001;304–306:1.